ELSEVIER

Thermochimica Acta 325 (1999) 35–41

thermochimica acta

Thermal and spectral studies of 3-*N*-methyl-morpholino-4-amino-5-mercapto-1,2,4-triazole and 3-*N*-methyl-piperidino-4-amino-5-mercapto-1,2,4-triazole complexes of cobalt(II), nickel(II) and copper(II)

P.B. Maravalli, T.R. Goudar*

P.G. Department of studies in Chemistry, Karnatak University, Dharwad-580 003, India

Received 2 September 1998; received in revised form 11 September 1998; accepted 15 September 1998

Abstract

Novel complexes obtained by 3-*N*-methyl-morpholino-4-amino-5-mercapto-1,2,4-triazole and 3-*N*-methyl-piperidino-4-amino-5-mercapto-1,2,4-triazole with Co(II), Ni(II) and Cu(II) have been synthesized and characterized by elemental analysis, electronic, IR, ESR and TG studies. TG studies of these complexes showed that thermal degradation proceeds in two steps. Kinetic and thermodynamic parameters were computed from the thermal decomposition data. The activation energy of both the thermal degradation steps is in the 0.22–44.67 kJ mol^{-1} range. Based on the spectral and TG studies, an octahedral geometry can be proposed for the above complexes.

Keywords: Complexes; Synthesis; Thermal degradation; Thermodynamic; Thermogravimetry

1. Introduction

In recent years, there has been considerable interest in the complexes formed by oxadiazole, triazole and related ligands as they are common components of some important biological molecules [1,2]. Furthermore, triazoles have been reported to possess a wide range of biological activities, including antibacterial, antifungal, antitumour and antiviral [3–6].

Thermal decomposition parameters, such as E, ln A, $\Delta H^{\#}$, $\Delta S^{\#}$ and $\Delta G^{\#}$ have been derived for transition-metal complexes of various classes of organic ligands [7–13]. However, very little work has been done on triazole–metal complexes of transition elements. Hence, the present paper reports the synthesis, spectral and thermal studies of new cobalt(II), nickel(II) and copper(II) complexes derived from 3-*N*-methyl-morpholino-4-amino-5-mercapto-1,2,4-triazole (MMAMT) and 3-*N*-methyl-piperidino-4-amino-5-mercapto-1,2,4-triazole(MPAMT). Kinetic and thermodynamic parameters have been calculated using Broido's relation [14].

2. Experimental

All the chemical and solvents used were of AR grade.

2.1. Synthesis of ligands

The ligands 3-*N*-methylmorpholino-4-amino-5-mercapto-1,2,4-triazole (MMAMT) and 3-*N*-methyl-

*Corresponding author. Fax: +1-91-836 747884; e-mail: Karuni@bom2.vsnl.net.in

0040-6031/99/$ – see front matter
PII: S0040-6031(98)00548-6

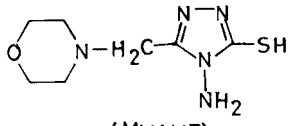

(MMAMT)

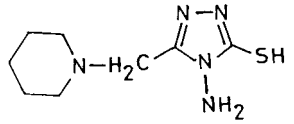

(MPAMT)

Fig. 1. Structure of ligands MMAMT and MPAMT.

piperidino-4-amino-5-mercapto-1,2,4-triazole (MPAMT) (Fig. 1) were prepared and purified according to the methods reported in the literature [15].

2.2. Synthesis of complexes

Metal(II) chloride (0.01 mol) was treated with the ligand (0.01 mol) in alcoholic medium. The reaction mixture was refluxed for about one hour and then 2 g of sodium acetate was added to the reaction mixture and refluxed for ca. 3 h. The separated complex was filtered, washed with aqueous alcohol followed by absolute alcohol and finally dried in vacuum over fused calcium chloride.

2.3. Analytical methods

Metal in the complexes were analysed according to the standard procedures [16]. Magnetic moments were measured using Gouy balance. Conductance measurements were made using 10^{-3} M solutions of the complexes in DMF with the help of Elico conductivity bridge type CM-82. IR spectra of the ligands and the corresponding complexes were recorded in Nicolet Impact 410 spectrophotometer using KBr pellets. A Hitachi 150-20 spectrophotometer was used for recording the electronic spectra. The ESR spectra were recorded on a EPR-E-4 spectrometer, operating in the *x*-band region with TCNE as the reference material at 300 and 77 K. Thermal studies were carried out with a Rigaku TAS-100 Model thermal analyser. A 5–8 mg pure sample was subjected to dynamic TG scans at a heating rate of 10°C min^{-1} in an air atmosphere, in the temperature range from ambient to 900°C. The TG curves were analysed as percentage mass loss as a function of temperature. The number of decomposition steps were identified using DTG. The activation energy (E_a) and frequency factor ($\ln A$) of the degradation process were obtained by Broido's method [14].

3. Results and discussion

All the prepared complexes are crystalline, non-hygroscopic, insoluble in non-polar solvents. However, they are soluble in polar solvents like DMF and DMSO. The molar conductance values fall in the 2.54–9.78 Ω^{-1} mol^{-1} cm^2 range which suggests the non-electrolytic nature of the complexes. The analytical data reveals 1 : 1 stoichiometry between metal : -ligand (Table 1). The magnetic moment data of Co(II), Ni(II) and Cu(II) complexes shown in Table 1 reveals distorted octahedral geometry. However, the subnormal magnetic moment in Cu(II) complex indicates copper–copper interaction leading to polymeric nature [17,18].

3.1. Electronic spectra

The electronic spectra of Co(II) complexes shows two *d*–*d* bands in the 19 600–20 830 and 7849–8130 cm^{-1} ranges which could be assigned to $^4T_{1g}(P) \leftarrow {}^4T_{1g}(F)$ and $^4T_{2g}(F) \leftarrow {}^4T_{1g}(F)$ transitions confirming octahedral geometry for these complexes [19].

The visible spectrum of the nickel(II) complexes exhibits three bands at 8696–8969 cm^{-1}, 14 368–15 267 cm^{-1} and 23 529–24 096 cm^{-1}, attributed to the transitions $^3T_{2g}(F) \leftarrow {}^3A_{2g}(F)$, $^3T_{1g}(F) \leftarrow {}^3A_{2g}(F)$ and $^3T_{1g}(P) \leftarrow {}^3A_{2g}(F)$, respectively. This reveals the octahedral geometry around nickel(II) ion [20]. The electronic spectra of copper(II) complexes show a very broad band of low intensity in the 17 200–17 391 cm^{-1} region, which can be assigned to the $^2T_{2g} \leftarrow {}^2E_g$ transition. In addition to this band, another band is also seen in the 23 529–24 691 cm^{-1} region. This band is due to symmetry forbidden ligand→metal charge transfer. The band above 27 000 cm^{-1} is assigned as ligand band. Distorted octahedral structures are proposed on the basis of electronic spectra.

Table 1
Analytical, magnetic and conductivity data of Co(II), Ni(II) and Cu(II) complexes with MMAMT and MPAMT

S. No.	Complex	Elemental analysis %						Molar conductance,λM	Magnetic moment (μB)
		C	H	N	S	Cl	M	Ω^{-1} mol^{-1} cm^2	
1	[Co(MMAMT)Cl·2H$_2$O]	24.46 (24.38)	3.62 (3.48)	20.28 (20.33)	9.18 (9.28)	10.25 (10.39)	16.94 (17.12)	2.54	4.30
2	[Ni(MMAMT)Cl·2H$_2$O]	24.70 (24.42)	3.84 (3.48)	20.42 (20.34)	9.25 (9.39)	10.64 (10.36)	17.24 (17.05)	7.74	3.10
3	[Cu(MMAMT)Cl·H$_2$O]	25.46 (25.36)	3.42 (3.65)	20.42 (21.19)	9.60 (9.66)	10.55 (10.72)	19.12 (19.30)	2.17	1.32
4	[Co(MPAMT)Cl·2H$_2$O]	28.12 (28.09)	3.90 (4.09)	27.98 (20.46)	9.38 (9.40)	10.24 (10.37)	17.16 (17.22)	8.76	4.27
5	[Ni(MPAMT)Cl·2H$_2$O]	28.36 (28.07)	4.18 (4.09)	20.82 (20.46)	9.30 (9.40)	9.78 (10.37)	18.02 (18.12)	6.41	2.93
6	[Cu(MPAMT)Cl·H$_2$O]	28.92 (29.19)	4.12 (4.00)	20.65 (21.27)	9.65 (9.72)	10.56 (10.79)	20.24 (19.46)	9.78	0.86

3.2. Infrared spectra

The ligands MMAMT and MPAMT show resolved bands at 3271, 3141 and 2570 cm^{-1}. These bands have been assigned to $\nu_{(NH)}$ and $\nu_{(SH)}$ [15] modes, respectively. The high intensity bands in the 1622–1604 cm^{-1} and 1579–1567 cm^{-1} regions can be assigned to >C=N stretching frequencies. The two strong bands at 1510 and 1307 cm^{-1} have been respectively assigned to thioamide bands [21] I and II. A medium-intensity band at 900 cm^{-1} is assigned to N–N stretching vibration. The thioamide band IV which is mainly due to >C=S stretching vibration is observed at 750 cm^{-1}.

The IR spectra of metal(II) complexes with the above-mentioned ligands show a broad band around 3430 cm^{-1} which is due to ν(OH) of coordinated water. The NH stretching frequencies observed at 3271 cm^{-1} in the ligand has shifted to 3221 cm^{-1} in the complexes suggesting the coordination of amino group to metal(II) ion. The $\nu_{(C=N)}$ vibration observed in the 1622–1604 and 1579–1567 cm^{-1} regions in the spectrum of the ligand show some changes in the complexes. A broad band, with halfwidth ca. 70 cm^{-1} is observed around 1630 cm^{-1}. This observation indicates the coordination of one of the azomethine groups to the metal atom through nitrogen which results in a shift of the 1579 cm^{-1} band due to higher wave number. The band due to $\nu_{(C=S)}$ would shift towards lower wave numbers on complexation. Both these effects are actually observed since the thioamide band which has a major contribution from $\nu_{(C=N)}$ and a minor contribution from $\nu_{(C–N)}$, appearing at 1307 cm^{-1}, in the spectrum of the ligand, shifts by 60 cm^{-1} towards higher wave numbers in the complexes. The thioamide at 750 cm^{-1} in the ligand, which is mostly due to $\nu_{(C=S)}$, shifts by 80–70 cm^{-1} towards lower wave numbers on complexation [22].

3.3. Electron spin resonance spectra

In the ESR spectra, from the observed 'g' values of Cu(II) complexes at LNT ($g_{\|}$=2.289, $g_{\perp}$=2.103), it is evident that the unpaired electron is predominantly in $d_{x^2-y^2}$ orbital with the possibility of some d_{z^2} character being mixed with it because of low symmetry. The $g_{\|}$ value ($g_{\|}$=2.289<2.3) indicates a larger percentage of covalency. The G value (G=2.8) of less than four concludes interaction between copper centres, which is further supported by the subnormal magnetic moment. The relation $g_{\|}>g_{\perp}>2.0$ in the present case suggests an elongated octahedral geometry [23].

Table 2
Thermogravimetric characteristics of Co(II), Ni(II) and Cu(II) complexes of MMAMT and MPAMT

Complex	Process	Temperature range/°C	Product	Mass%		No.of moles	Residue %		Nature
				calc	expt		calc	expt	
[Co(MMAMT)Cl·2H_2O]	dehydration and		H_2O and			2			
	decomposition	40–280	Cl	20.74	20.04	1			
	of coordination sphere (L, Cl)	281–640	L	62.11	61.74	1	24.14	24.34	Co_3O_4
[Ni(MMAMT)Cl·2H_2O]	dehydration and		H_2O and			2			
	decomposition	35–250	Cl	20.78	21.28	1			
	of coordination sphere (L, Cl)	251–580	L	62.74	62.83	1	22.00	22.15	NiO
[Cu(MMAMT)Cl·H_2O]	dehydration and		H_2O and			1			
	decomposition	40–262	Cl	16.16	16.70	1			
	of coordination sphere (L, Cl)	263–688	L	65.25	65.84	1	25.35	25.50	CuO
[Co(MPAMT)Cl·2H_2O]	dehydration and		H_2O and			2			
	decomposition	40–230	Cl	20.87	19.74	1			
	of coordination sphere (L, Cl)	231–850	L	62.18	61.41	1	24.87	24.15	Co_3O_4
[Ni(MPAMT)Cl·2H_2O]	dehydration and		H_2O and			2			
	decomposition	50–220	Cl	19.95	20.10	1			
	of coordination sphere (L, Cl)	221–550	L	61.74	62.41	1	22.67	22.72	NiO
[Cu(MPAMT)Cl·H_2O]	dehydration and		H_2O and			1			
	decomposition	70–310	Cl	16.76	16.04	1			
	of coordination sphere (L, Cl)	311–720	L	64.75	63.84	1	24.55	24.75	CuO

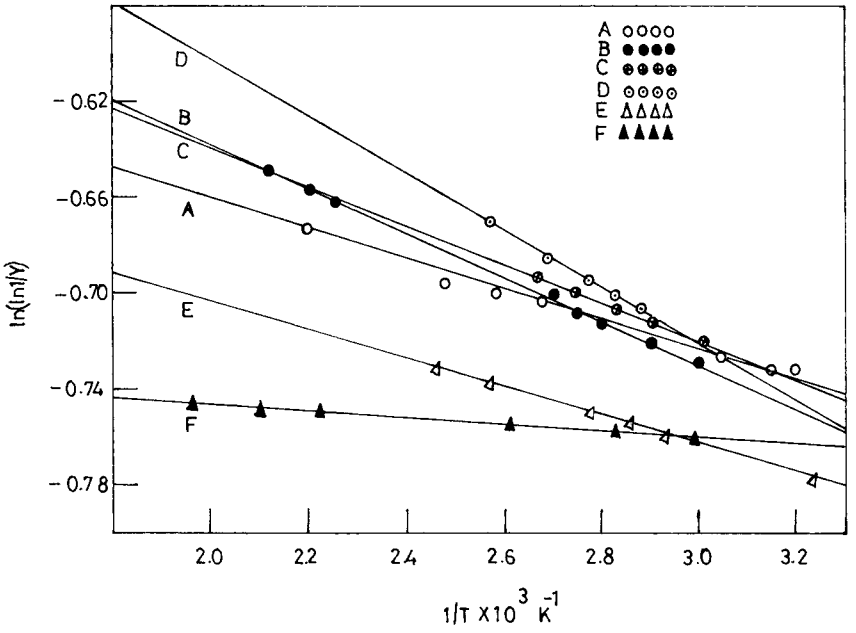

Fig. 2. Plots of ln (ln 1/*y*) vs. 1/*T* for the first degradation process of: (A) [Co(MMAMT)Cl·2H_2O]; (B) [Ni(MMAMT)Cl·2H_2O]; (C) [Cu(MMAMT)Cl·H_2O]; (D) [Co(MPAMT)Cl·2H_2O]; (E) [Ni(MPAMT)Cl·2H_2O]; and (F) [Cu(MPAMT)Cl·H_2O].

3.4. Thermal analysis

The temperature of decomposition, the pyrolysed products, the percentage mass loss of the ligands, and the percent ash are given in Table 2.

All the complexes decompose in two steps. The first step, 35–310°C, brings about a mass loss ranging between 16.2 and 20.1%. This loss corresponds to a loss of one coordinated water and chloride as HCl. In the second step of decomposition the ligand is lost in the 211–850°C range. There is no further mass loss beyond 850°C and a plateau is obtained which corresponds to the formation of a stable metal oxide. It agrees well with analytical results within the experimental errors.

The measured curves obtained during TG scans were analysed to give the percentage mass loss as a function of temperature. T_0 (temperature of onset of decomposition), T_{10} (temperature for 10% mass loss) and T_{max} (temperature of maximum mass loss) are the main criteria to indicate the thermal stability of the complexes. The higher the values of T_0, T_{10} and T_{max}, the higher the thermal stability.

Broido's method was used to evaluate the kinetic parameters from the TG curve. Plots of ln (ln 1/*y*) vs. 1/*T* (where *y* is the fraction not yet decomposed) for different stages of the thermal degradation process of the complexes were identified and are shown in Figs. 2 and 3. Fig. 2 represents the first step of degradation and Fig. 3 the second.

In order to determine the thermal stability trend, the parameters T_0, T_{10}, T_{max}, the activation energy (E_a) and the frequency factor (ln *A*), were evaluated and are given in Table 3. The thermodynamic parameters, enthalpy ($\Delta H^{\#}$), entropy ($\Delta S^{\#}$) and free energy ($\Delta G^{\#}$) of activation were calculated using standard equations and the values are given in Table 4.

The $\Delta S^{\#}$ values were found to be negative, which indicates a more ordered activated state that may be possible through the chemisorption of oxygen and other decomposition products [24]. The values of activation energy for the second stage of decomposition were found to be higher than that for the first stage which indicates that the rate of decomposition of the second stage is lower than that of first stage. This may be attributed to the structural rigidity of the ligand, 3-*N*-methyl-morpholino-4-amino-5-mercapto-1,2,4-triazole and 3-*N*-methyl-piperidino-4-amino-5-mercapto-1,2,4-triazole, as compared with H_2O and Cl, which requires more energy for its rearrangement

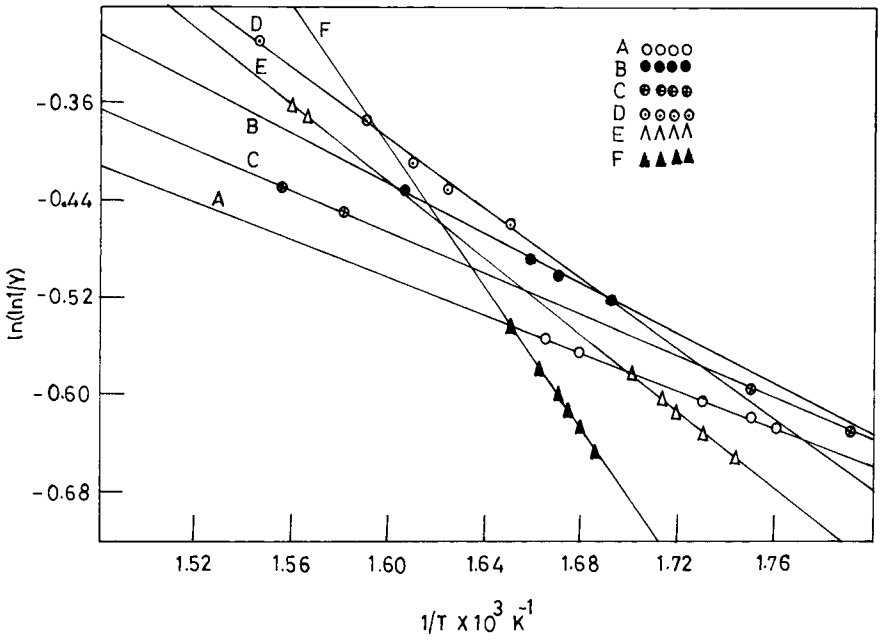

Fig. 3. Plots of ln (ln 1/*y*) vs. 1/*T* for the second degradation process of: (A) [Co(MMAMT)Cl·2H_2O]; (B) [Ni(MMAMT)Cl·2H_2O]; (C) [Cu(MMAMT)Cl·H_2O]; (D) [Co(MPAMT)Cl·2H_2O]; (E) [Ni(MPAMT)Cl·2H_2O]; and (F) [Cu(MPAMT)Cl·H_2O].

before undergoing any compositional change. Further, it is generally observed that stepwise formation constants decrease with an increase in the number of ligands attached to the metal ion [25]. During the decomposition reactions a reverse effect may occur. Hence, the rate of removal of the remaining ligands will be smaller after the expulsion of one or two ligands [26].

Table 3
Data obtained from TGA analysis: temperature characteristics, activation energies and frequency factors of the decomposition process

Complex	T_0/°C	T_{10}/°C	T_{max}/°C	Process	E_a/(kJ mol^{-1})	ln [A/min^{-1}]
[Co(MMAMT)Cl·2H_2O]	40	210	640	I	0.95	4.34
				II	12.44	9.17
[Ni(MMAMT)Cl·2H_2O]	35	125	580	I	1.66	5.14
				II	12.12	9.25
[Cu(MMAMT)Cl·H_2O]	40	220	688	I	1.53	5.02
				II	14.67	9.90
[Co(MPAMT)Cl·2H_2O]	40	98	850	I	2.17	5.60
				II	27.52	13.02
[Ni(MPAMT)Cl·2H_2O]	50	220	580	I	1.14	4.56
				II	30.63	5.91
[Cu(MPAMT)Cl·H_2O]	70	285	720	I	0.22	2.60
				II	44.67	16.94

Table 4
Thermogravimetric parameters for the thermal degradation of the process

Complex	Process	$\Delta H^{\#}$/(kJ mol^{-1})	$\Delta S^{\#}$/(J K^{-1} mol^{-1})	$\Delta G^{\#}$/(kJ mol^{-1})
[Co(MMAMT)Cl·2H$_2$O]	I	−2.26	−150.90	56.13
	II	7.18	−126.82	87.46
[Ni(MMAMT)Cl·2H$_2$O]	I	−1.35	−149.41	50.67
	II	7.26	−126.77	81.42
[Cu(MMAMT)Cl·H$_2$O]	I	−1.48	−149.69	52.85
	II	9.72	−122.89	82.96
[Co(MPAMT)Cl·2H$_2$O]	I	−0.76	−147.99	51.47
	II	22.36	−100.63	84.85
[Ni(MPAMT)Cl·2H$_2$O]	I	−1.75	−151.57	51.47
	II	25.45	−87.73	80.11
[Cu(MPAMT)Cl·H$_2$O]	I	−3.50	−152.25	64.70
	II	39.67	−73.85	84.06

The values of the entropy for all degradation steps of all the complexes are negative. The enthalpies of activation are negative for the first step and positive for the second. However, the negative values of the entropies of activation are compensated by the values of the enthalpies of activation, leading to almost the same values (50.67–87.46 kJ mol^{-1}) for the free energies of activation.

References

[1] V. Dwivedi, R.K. Agarwal, Indian J. Pharm. Sci. 53 (1991) 82.
[2] L. Mishra, V.K. Singh, N.K. Dubey, A.K. Mishra, Biosci. Biotech. Biochem. 57 (1993) 989.
[3] P.H. Freeman, P.A. Worthington, W.G. Rathmell, Eur. Pat. Appl. EP 0044, (1982) 407.
[4] J.L. Hilton, J. Agric. Food Chem. 17 (1969) 182.
[5] C.K. Joshi, K. Dubey, Phamazie 34 (1979) 801.
[6] L. Mishra, M. Kamil Said, Indian J. Chem. 35A (1996) 304.
[7] R.K. Agrawal, S.C. Rastogi, Thermochim. Acta 63 (1983) 363.
[8] V.V. Savant, P. Ramamurthy, C.C. Patel, J. Less Common Metals 22 (1970) 479.
[9] A.K. Srivastava, S. Sharma, R.K. Agrawal, Inorg. Chim. Acta 61 (1982) 235.
[10] K. Arora, Asian J. Chem. 7 (1995) 508.
[11] N.S. Bhave, V.S. Iyer, J. Therm. Anal. 32 (1987) 1369.
[12] N. Calu, L. Odochian, G.L. Brinzan, N. Bilba, J. Therm. Anal. 30 (1985) 547.
[13] H.S. Bhojya Naik, Siddaramaiah, P.G. Ramappa, Thermochim. Acta, 2998 (1996).
[14] A. Broido, J. Polym. Sci., Part A-2 7 (1969) 1761.
[15] M.C. Hosur, M.B. Talawar, S.C. Bennur, Indian J. Chem. 34B (1995) 707.
[16] A.I. Vogel, A Text Book of Quantitative Inorganic Analysis, Longmans Green, London, 1968.
[17] B.C. Bahl, B.L. Dubey, N. Nath, A. Tripathi, J.K. Srivastav, J. Indian Chem. Soc. 59 (1982) 1127.
[18] R.C. Varma, K. Varma, R.K. Varma, N.C. Bhattacharjee, J. Indian Chem. Soc. 69 (1992) 577.
[19] A.B.P. Lever, Inorganic Electronic Spectroscopy, Elserier, New York, 1968, pp. 333.
[20] C.J. Ballhausen, Introduction to Ligand Field Theory, McGraw Hill, New York, 1962.
[21] B.M. Badiger, S.A. Patil, S.M. Kudari, V.H. Kulkarni, Revue Roumaine de Chimie 31 (1986) 849.
[22] B.K. Gupta, D.S. Gupta, S.K. Dikshit, U. Agarwala, Indian J. Chem., 15A (1987) 1021.
[23] G. Wilkinson, Comprehensive Coordination Chemistry, Pergmon press, 5 (1987) 663.
[24] P.M. Madhusudanan, K.K.M. Yusuff, C.G.R. Nair, J. Therm. Anal. 8 (1975) 31.
[25] F.A. Cotton, G. Wilkinson, Advanced Inorganic Chemistry, Wiley Interscience, New York, 1988.
[26] K.K.M. Yusuff, R. Sreekala, Thermochim. Acta 159 (1990) 357.